4984 *Inorg. Chem.* **2010**, *49*, 4984–4995
DOI: 10.1021/ic100092d

Inorganic Chemistry
Article

Design of Luminescent Biotinylation Reagents Derived from Cyclometalated Iridium(III) and Rhodium(III) Bis(pyridylbenzaldehyde) Complexes

Siu-Kit Leung, Karen Ying Kwok, Kenneth Yin Zhang, and Kenneth Kam-Wing Lo*

Department of Biology and Chemistry, City University of Hong Kong, Tat Chee Avenue, Kowloon, Hong Kong, People's Republic of China

Received January 16, 2010

A new class of luminescent biotinylation reagents derived from cyclometalated iridium(III) and rhodium(III) bis(pyridylbenzaldehyde) biotin complexes, $[Ir(pba)_2(bpy\text{-}C6\text{-}biotin)](PF_6)$ (**1**), $[Ir(pba)_2(bpy\text{-}TEG\text{-}biotin)](PF_6)$ (**2**), and $[Rh(pba)_2(bpy\text{-}C6\text{-}biotin)](PF_6)$ (**3**), together with their biotin-free counterparts $[Ir(pba)_2(bpy\text{-}Et)](PF_6)$ (**4**) and $[Rh(pba)_2(bpy\text{-}Et)](PF_6)$ (**5**) [Hpba = 4-(2-pyridyl)benzaldehyde, bpy-C6-biotin = 4-[(6-biotinamido)hexylaminocarbonyl]-4′-methyl-2,2′-bipyridine, bpy-TEG-biotin = 4-[(13-biotinamido-4,7,10-trioxa)tridecylaminocarbonyl]-4′-methyl-2,2′-bipyridine, bpy-Et = 4-(ethylaminocarbonyl)-4′-methyl-2,2′-bipyridine], have been synthesized and characterized and their photophysical and electrochemical properties studied. Upon photoexcitation, the iridium(III) complexes **1**, **2**, and **4** exhibited intense and long-lived orange-yellow luminescence in fluid solutions at 298 K and in rigid glass at 77 K. The rhodium(III) complexes **3** and **5** were weakly emissive in fluid solutions at 298 K but showed intense luminescence in low-temperature glass. In view of the structured emission profiles and the long lifetimes, the emission of all of the complexes has been assigned to a triplet intraligand (^{3}IL) ($\pi \rightarrow \pi^*$) (pba) excited state, which was probably mixed with some triplet metal-to-ligand charge-transfer (^{3}MLCT) [dπ(Ir or Rh) $\rightarrow \pi^*$(pba)] character. To investigate the reactivity of the aldehyde groups, complex **2** was reacted with *n*-butylamine, resulting in the formation of the complex $[Ir(ppy\text{-}CH_2NHC_4H_9)_2(bpy\text{-}TEG\text{-}biotin)](PF_6)$ (**2a**) [Hppy-$CH_2NHC_4H_9$ = 2-[4-[*N*-(*n*-butyl)aminomethyl]phenyl]pyridine]. All of the aldehyde complexes have been used to biotinylate bovine serum albumin (BSA) to form bioconjugates **1-BSA**−**5-BSA**. The bioconjugates have been isolated, purified, and characterized and their photophysical properties studied. Upon photoexcitation, all of the bioconjugates were luminescent and the emission has been attributed to a ^{3}MLCT [dπ(Ir) $\rightarrow \pi^*$(N^N)] state for the iridium(III) conjugates and a mixed ^{3}IL ($\pi \rightarrow \pi^*$) (N^N and N^C)/^{3}MLCT [dπ(Rh) $\rightarrow \pi^*$(N^N)] state for the rhodium(III) conjugates. The avidin-binding properties of complexes **1**, **2**, **2a**, and **3** and bioconjugates **1-BSA**−**3-BSA** have been investigated using the 4′-hydroxyazobenzene-2-carboxylic acid assay. Emission titrations showed that complex **2a** displayed a significant change of the emission profile upon binding to avidin. Additionally, the cytotoxicity of all of the iridium(III) and rhodium(III) complexes toward the human cervix epithelioid carcinoma cells has been examined by the 3-(4,5-dimethyl-2-thiazolyl)-2,5-diphenyltetrazolium bromide assay. Furthermore, the cellular uptake properties of the complexes and bioconjugate **2-BSA** have been investigated by laser-scanning confocal microscopy.

Introduction

Modification of biomolecules with a biotin (biotinylation) is widely applied in the purification, recognition, and immobilization of biomolecules owing to the rapid, strong, and specific avidin−biotin interactions.[1−4] One advantage is that the biological characteristics and properties of common biomolecules are usually retained after biotinylation. Thus, a wide range of biotinylation reagents that are reactive toward different functional groups of biomolecules have been designed, and many of them are already commercially available.[3] To optimize avidin−biotin assays and to maintain the labeling reproducibility, the degree of biotinylation of the biomolecules must be known. This is routinely determined by the 4′-hydroxyazobenzene-2-carboxylic acid (HABA) assay, which is based on the decrease of absorption due to the displacement of avidin-bound HABA molecules

*To whom correspondence should be addressed. E-mail: bhkenlo@cityu.edu.hk. Tel: (852) 2788 7231. Fax: (852) 2788 7406.

(1) (a) Green, N. M. *Adv. Protein Chem.* **1975**, *29*, 85–133. (b) Green, N. M. *Methods Enzymol.* **1990**, *184*, 51–67.

(2) (a) Wilchek, M.; Bayer, E. A. *Anal. Biochem.* **1988**, *171*, 1–32. (b) Wilchek, M.; Bayer, E. A. *Methods Enzymol.* **1990**, *184*, 123–138.

(3) (a) Savage, M. D.; Mattson, G.; Desai, S.; Nielander, G. W.; Morgensen, S.; Conklin, E. J. *Avidin-Biotin Chemistry: A Handbook*; Pierce Chemical Company: Rockford, IL, 1992. (b) Thermo Fisher Scientific Inc. *Thermo Scientific Avidin-Biotin Technical Handbook*, http://www.piercenet.com/files/1601675_AvBi_HB_INTL.pdf.

(4) Hermanson, G. T. *Bioconjugate Techniques*; Academic Press: San Diego, CA, 1996.

Published on Web 05/13/2010

($\varepsilon_{500\ nm}$ = 34 000 dm^3 mol^{-1} cm^{-1}) by the biotinylated species.[1a,4] Additionally, there are commercially available chromogenic biotinylation reagents such as biotin-X 2,4-dinitrophenyl-X-L-lysine NHS ester[5a] ($\varepsilon_{364\ nm}$ = 15 000 dm^3 mol^{-1} cm^{-1}), EZ-Link NHS-chromogenic-biotin[5b] ($\varepsilon_{354\ nm}$ = 29 000 dm^3 mol^{-1} cm^{-1}), and its structural analogues,[5c] which enable spectrophotometric quantitation of the extent of biotinylation. Luminescent biotinylation reagents are attractive candidates because more sensitive spectrofluorometric methods can be employed to determine the level of biotinylation. Additionally, the luminescence properties of the biotinylated biomolecules may lead to the design of new bioassays, and the biological uptake of the biotinylated biomolecules can be investigated by luminescence spectroscopy and microscopy. Furthermore, biotinylation of small molecular substrates can allow the isolation and purification of the specific biological receptors by affinity chromatography coupled with luminescence detection. We have recently reported the first design of luminescent biotinylation reagents based on rhenium(I) polypyridine complexes.[6a] Related fluorescent organic biotinylation reagents have also been described very recently.[6b] Additionally, we have exploited luminescent cyclometalated iridium(III) and rhodium(III) bis(pyridylbenzaldehyde) complexes as biological labeling reagents.[7] Thus, in view of the interesting emission properties of luminescent iridium(III) and rhodium(III) complexes,[7−30] we believe that they are attractive candidates to be developed as new luminescent biotinylation reagents.

Herein, we describe a new class of luminescent biotinylation reagents derived from cyclometalated iridium(III) and rhodium(III) bis(pyridylbenzaldehyde) biotin complexes, [Ir(pba)$_2$(bpy-C6-biotin)](PF$_6$) (**1**), [Ir(pba)$_2$(bpy-TEG-biotin)](PF$_6$) (**2**), and [Rh(pba)$_2$(bpy-C6-biotin)](PF$_6$) (**3**), together

(5) (a) Haugland, R. P. *The Handbooks: A Guide to Fluorescent Probes and Labeling Technologies*, 10th ed.; Molecular Probes, Inc.: Eugene, OR, 2005; section 1.2. See: http://probes.invitrogen.com/handbook/sections/0102.html. (b) Pierce Chemical Co. Product Catalog, http://www.piercenet.com/files/1780as4.pdf. (c) The Conjugation Co. SoluLink, http://www.solulink.com/products.php?action=search&srchID=6.

(6) (a) Lo, K. K.-W.; Louie, M.-W.; Sze, K.-S.; Lau, J. S.-Y. *Inorg. Chem.* **2008**, *47*, 602–611. (b) Garanger, E.; Weissleder, R.; Josephson, L. *Bioconjugate Chem.* **2009**, *20*, 170–173.

(7) (a) Lo, K. K.-W.; Chung, C.-K.; Zhu, N. *Chem.—Eur. J.* **2003**, *9*, 475–483. (b) Lo, K. K.-W.; Li, C.-K.; Lau, K.-W.; Zhu, N. *Dalton Trans.* **2003**, 4682–4689. (c) Lo, K. K.-W.; Hui, W.-K.; Chung, C.-K.; Tsang, K. H.-K.; Ng, D. C.-M.; Zhu, N.; Cheung, K.-K. *Coord. Chem. Rev.* **2005**, *249*, 1434–1450.

(8) (a) Sprouse, S.; King, K. A.; Spellane, P. J.; Watts, R. J. *J. Am. Chem. Soc.* **1984**, *106*, 6647–6653. (b) King, K. A.; Spellane, P. J.; Watts, R. J. *J. Am. Chem. Soc.* **1985**, *107*, 1431–1432. (c) King, K. A.; Watts, R. J. *J. Am. Chem. Soc.* **1987**, *109*, 1589–1590. (d) Ohsawa, Y.; Sprouse, S.; King, K. A.; DeArmond, M. K.; Hanck, K. W.; Watts, R. J. *J. Phys. Chem.* **1987**, *91*, 1047–1054.

(9) (a) Didier, P.; Ortmans, I.; Kirsch-De Mesmaeker, A.; Watts, R. J. *Inorg. Chem.* **1993**, *32*, 5239–5245. (b) Ortmans, I.; Didier, P.; Kirsch-De Mesmaeker, A. *Inorg. Chem.* **1995**, *34*, 3695–3704. (c) Ghizdavu, L.; Lentzen, O.; Schumm, S.; Brodkorb, A.; Moucheron, C.; Kirsch-De Mesmaeker, A. *Inorg. Chem.* **2003**, *42*, 1935–1944.

(10) Nonoyama, M.; Yamasaki, K. *Inorg. Nucl. Chem. Lett.* **1971**, *7*, 943–946.

(11) (a) Maestri, M.; Sandrini, D.; Balzani, V.; Maeder, U.; von Zelewsky, A. *Inorg. Chem.* **1987**, *26*, 1323–1327. (b) Sandrini, D.; Maestri, M.; Balzani, V.; Maeder, U.; von Zelewsky, A. *Inorg. Chem.* **1988**, *27*, 2640–2643. (c) Barigelletti, F.; Sandrini, D.; Maestri, M.; Balzani, V.; von Zelewsky, A.; Chassot, L.; Jolliet, P.; Maeder, U. *Inorg. Chem.* **1988**, *27*, 3644–3647.

(12) (a) Zilian, A.; Maeder, U.; von Zelewsky, A.; Güdel, H. U. *J. Am. Chem. Soc.* **1989**, *111*, 3855–3859. (b) Colombo, M. G.; Zilian, A.; Güdel, H. U. *J. Am. Chem. Soc.* **1990**, *112*, 4581–4582. (c) Frei, G.; Zilian, A.; Raselli, A.; Güdel, H. U.; Bürgi, H.-B. *Inorg. Chem.* **1992**, *31*, 4766–4773.

(13) (a) Erkkila, K. E.; Odom, D. T.; Barton, J. K. *Chem. Rev.* **1999**, *99*, 2777–2796. (b) Kisko, J. L.; Barton, J. K. *Inorg. Chem.* **2000**, *39*, 4942–4949.

(14) (a) Holder, E.; Marin, V.; Kozodaev, D.; Meier, M. A. R.; Lohmeijer, B. G. G.; Schubert, U. S. *Macromol. Chem. Phys.* **2005**, *206*, 989–997. (b) Holder, E.; Marin, V.; Alexeev, A.; Schubert, U. S. *J. Polym. Sci., Polym. Chem.* **2005**, *43*, 2765–2776. (c) Marin, V.; Holder, E.; Hoogenboom, R.; Tekin, E.; Schubert, U. S. *Dalton Trans.* **2006**, 1636–1644.

(15) (a) Collin, J.-P.; Dixon, I. M.; Sauvage, J.-P.; Williams, J. A. G.; Barigelletti, F.; Flamigni, L. *J. Am. Chem. Soc.* **1999**, *121*, 5009–5016. (b) Dixon, I. M.; Collin, J.-P.; Sauvage, J.-P.; Flamigni, L.; Encinas, S.; Barigelletti, F. *Chem. Soc. Rev.* **2000**, *29*, 385–391. (c) Auffrant, A.; Barbieri, A.; Barigelletti, F.; Lacour, J.; Mobian, P.; Collin, J.-P.; Sauvage, J.-P.; Ventura, B. *Inorg. Chem.* **2007**, *46*, 6911–6919.

(16) (a) Neve, F.; La Deda, M.; Crispini, A.; Bellusci, A.; Puntoriero, F.; Campagna, S. *Organometallics* **2004**, *23*, 5856–5863. (b) Neve, F.; La Deda, M.; Puntoriero, F.; Campagna, S. *Inorg. Chim. Acta* **2006**, *359*, 1666–1672. (c) Nastasi, F.; Puntoriero, F.; Campagna, S.; Schergna, S.; Maggini, M.; Cardinali, F.; Delavaux-Nicot, B.; Nierengarten, J.-F. *Chem. Commun.* **2007**, 3556–3558.

(17) (a) Tamayo, A. B.; Alleyne, B. D.; Djurovich, P. I.; Lamansky, S.; Tsyba, I.; Ho, N. N.; Bau, R.; Thompson, M. E. *J. Am. Chem. Soc.* **2003**, *125*, 7377–7387. (b) Hirani, B.; Li, J.; Djurovich, P. I.; Yousufuddin, M.; Oxgaard, J.; Persson, P.; Wilson, S. R.; Bau, R.; Goddard, W. A., III; Thompson, M. E. *Inorg. Chem.* **2007**, *46*, 3865–3875. (c) Finkenzeller, W. J.; Hofbeck, T.; Thompson, M. E.; Yersin, H. *Inorg. Chem.* **2007**, *46*, 5076–5083.

(18) (a) De Angelis, F.; Fantacci, S.; Evans, N.; Klein, C.; Zakeeruddin, S. M.; Moser, J.-E.; Kalyanasundaram, K.; Bolink, H. J.; Grätzel, M.; Nazeeruddin, M. K. *Inorg. Chem.* **2007**, *46*, 5989–6001. (b) Di Censo, D.; Fantacci, S.; De Angelis, F.; Klein, C.; Evans, N.; Kalyanasundaram, K.; Bolink, H. J.; Grätzel, M.; Nazeeruddin, M. K. *Inorg. Chem.* **2008**, *47*, 980–989. (c) Baranoff, E.; Suàrez, S.; Bugnon, P.; Barolo, C.; Buscaino, R.; Scopelliti, R.; Zuppiroli, L.; Grätzel, M.; Nazeeruddin, Md. K. *Inorg. Chem.* **2008**, *47*, 6575–6577.

(19) (a) Wilkinson, A. J.; Goeta, A. E.; Foster, C. E.; Williams, J. A. G. *Inorg. Chem.* **2004**, *43*, 6513–6515. (b) Wilkinson, A. J.; Puschmann, H.; Howard, J. A. K.; Foster, C. E.; Williams, J. A. G. *Inorg. Chem.* **2006**, *45*, 8685–8699. (c) Williams, J. A. G.; Wilkinson, A. J.; Whittle, V. L. *Dalton Trans.* **2008**, 2081–2099. (d) Whittle, V. L.; Williams, J. A. G. *Inorg. Chem.* **2008**, *47*, 6596–6607.

(20) (a) Polson, M.; Fracasso, S.; Bertolasi, V.; Ravaglia, M.; Scandola, F. *Inorg. Chem.* **2004**, *43*, 1950–1956. (b) Polson, M.; Ravaglia, M.; Fracasso, S.; Garavelli, M.; Scandola, F. *Inorg. Chem.* **2005**, *44*, 1282–1289.

(21) (a) Coppo, P.; Duati, M.; Kozhevnikov, V. N.; Hofstraat, J. W.; De Cola, L. *Angew. Chem., Int. Ed.* **2005**, *44*, 1806–1810. (b) Orselli, E.; Kottas, G. S.; Konradsson, A. E.; Coppo, P.; Fröhlich, R.; De Cola, L.; van Dijken, A.; Büchel, M.; Börner, H. *Inorg. Chem.* **2007**, *46*, 11082–11093. (c) Mehlstäubl, M.; Kottas, G. S.; Colella, S.; De Cola, L. *Dalton Trans.* **2008**, 2385–2388. (d) Stagni, S.; Colella, S.; Palazzi, A.; Valenti, G.; Zacchini, S.; Paolucci, F.; Marcaccio, M.; Albuquerque, R. Q.; De Cola, L. *Inorg. Chem.* **2008**, *47*, 10509–10521.

(22) (a) Obara, S.; Itabashi, M.; Okuda, F.; Tamaki, S.; Tanabe, Y.; Ishii, Y.; Nozaki, K.; Haga, M. *Inorg. Chem.* **2006**, *45*, 8907–8921. (b) Yang, L.; Okuda, F.; Kobayashi, K.; Nozaki, K.; Tanabe, Y.; Ishii, Y.; Haga, M. *Inorg. Chem.* **2008**, *47*, 7154–7165.

(23) (a) Lowry, M. S.; Bernhard, S. *Chem.—Eur. J.* **2006**, *12*, 7970–7977. (b) Coughlin, F. J.; Westrol, M. S.; Oyler, K. D.; Byrne, N.; Kraml, C.; Zysman-Colman, E.; Lowry, M. S.; Bernhard, S. *Inorg. Chem.* **2008**, *47*, 2039–2048.

(24) (a) Chou, P.-T.; Chi, Y. *Chem.—Eur. J.* **2007**, *13*, 380–395. (b) Fang, C.-H.; Chen, Y.-L.; Yang, C.-H.; Chi, Y.; Yeh, Y.-S.; Li, E. Y.; Cheng, Y.-M.; Hsu, C.-J.; Chou, P.-T.; Chen, C.-T. *Chem.—Eur. J.* **2007**, *13*, 2686–2694. (c) Yang, C.-H.; Cheng, Y.-M.; Chi, Y.; Hsu, C.-J.; Fang, F.-C.; Wong, K.-T.; Chou, P.-T.; Chang, C.-H.; Tsai, M.-H.; Wu, C.-C. *Angew. Chem., Int. Ed.* **2007**, *46*, 2418–2421. (d) Chang, C.-F.; Cheng, Y.-M.; Chi, Y.; Chiu, Y.-C.; Lin, C.-C.; Lee, G.-H.; Chou, P.-T.; Chen, C.-C.; Chang, C.-H.; Wu, C.-C. *Angew. Chem., Int. Ed.* **2008**, *47*, 4542–4545.

(25) (a) Liu, S.-J.; Zhao, Q.; Chen, R.-F.; Deng, Y.; Fan, Q.-L.; Li, F.-Y.; Wang, L.-H.; Huang, C.-H.; Huang, W. *Chem.—Eur. J.* **2006**, *12*, 4351–4361. (b) Li, X.; Chen, Z.; Zhao, Q.; Shen, L.; Li, F.; Yi, T.; Cao, Y.; Huang, C. *Inorg. Chem.* **2007**, *46*, 5518–5527. (c) Liu, Z.; Nie, D.; Bian, Z.; Chen, F.; Lou, B.; Bian, J.; Huang, C. *ChemPhysChem* **2008**, *9*, 634–640. (d) Zhao, Q.; Li, L.; Li, F.; Yu, M.; Liu, Z.; Yi, T.; Huang, C. *Chem. Commun.* **2008**, 685–687.

(26) Dragonetti, C.; Falciola, L.; Mussini, P.; Righetto, S.; Roberto, D.; Ugo, R.; Valore, A.; De Angelis, F.; Fantacci, S.; Sgamellotti, A.; Ramon, M.; Muccini, M. *Inorg. Chem.* **2007**, *46*, 8533–8547.

(27) Zeng, X.; Tavasli, M.; Perepichka, I. F.; Batsanov, A. S.; Bryce, M. R.; Chiang, C.-J.; Rothe, C.; Monkman, A. P. *Chem.—Eur. J.* **2008**, *14*, 933–943.

(28) Freys, J. C.; Bernardinelli, G.; Wenger, O. S. *Chem. Commun.* **2008**, 4267–4269.

Chart 1. Structures of the Iridium(III) and Rhodium(III) Complexes

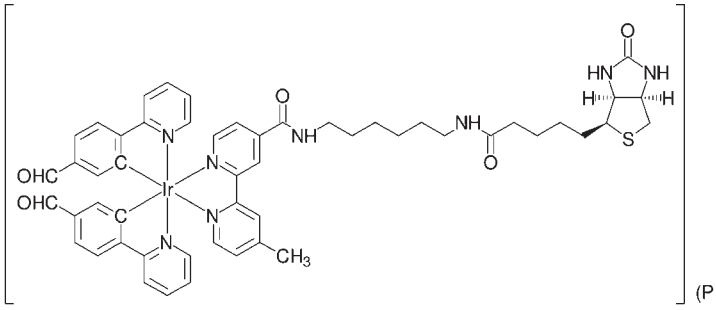

1

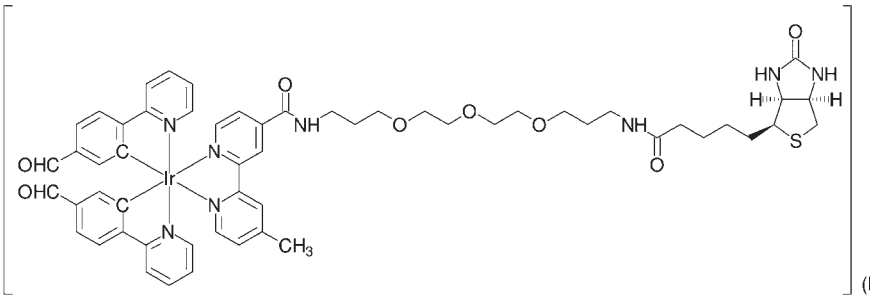

2

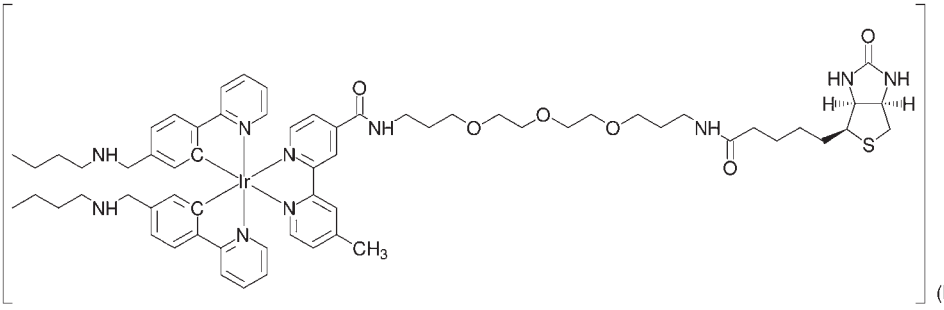

2a

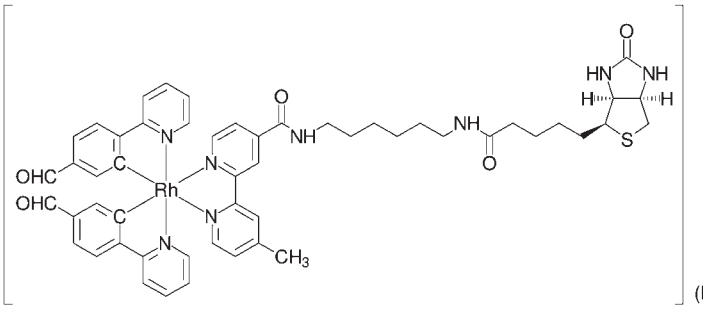

3

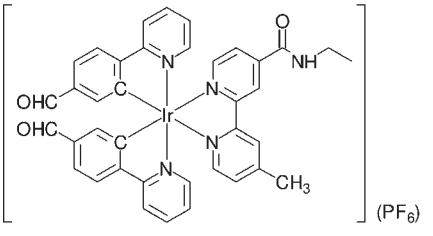

4

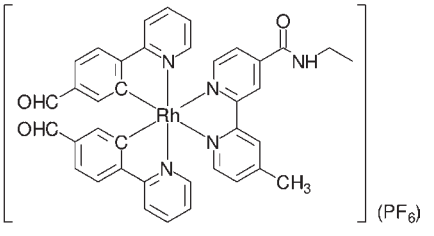

5

with their biotin-free counterparts $[Ir(pba)_2(bpy\text{-}Et)](PF_6)$ (**4**) and $[Rh(pba)_2(bpy\text{-}Et)](PF_6)$ (**5**) [Hpba = 4-(2-pyridyl)-benzaldehyde, bpy-C6-biotin = 4-[(6-biotinamido)hexylaminocarbonyl]-4′-methyl-2,2′-bipyridine, bpy-TEG-biotin = 4-[(13-biotinamido-4,7,10-trioxa)tridecylaminocarbonyl]-4′-methyl-2,2′-bipyridine, bpy-Et = 4-(ethylaminocarbonyl)-4′-methyl-2,2′-bipyridine; Chart 1]. To investigate the reactivity of the aldehyde groups, complex **2** was reacted with *n*-butylamine, resulting in the formation of the complex $[Ir(ppy\text{-}CH_2NHC_4H_9)_2(bpy\text{-}TEG\text{-}biotin)](PF_6)$ (**2a**) [Hppy-$CH_2NHC_4H_9$ = 2-[4-[*N*-(*n*-butyl)aminomethyl]phenyl]pyridine]. We have utilized the bis(pyridylbenzaldehyde) complexes as biotinylation reagents for bovine serum albumin (BSA). The conjugates have been isolated, purified, and characterized. Their emissive characteristics and avidin-binding properties have also been studied by spectroscopic methods. The cytotoxicity of the iridium(III) and rhodium(III) complexes toward the human cervix epithelioid carcinoma (HeLa) cells has been examined by the 3-(4,5-dimethylthiazol-2-yl)-2,5-diphenyltetrazolium bromide (MTT) assay. Furthermore, the cellular uptake properties of the complexes and bioconjugate **2-BSA** have been investigated by laser-scanning confocal microscopy.

Experimental Section

Materials and Synthesis. All solvents were of analytical grade and were purified according to standard procedures.[31] Buffer components were of biological grade and were used as received. Biotin, carbonyl cyanide 3-chlorophenylhydrazone (CCCP), *cis*-diamminedichloroplatinum(II) (cisplatin), ethylamine, *n*-butylamine, *N*,*N*′-dicyclohexylcarbodiimide, *N*-hydroxysuccinimide (NHS), $MgSO_4$, $NaBH_4$, $Na(CN)BH_4$, triethylamine, and trifluoroacetic acid were obtained from Acros. HABA and MTT were purchased from Sigma. Di-*tert*-butyl dicarbonate, Hpba, 4,4′-dimethyl-2,2′-bipyridine, *N*-Boc-1,6-diaminohexane hydrochloride, $IrCl_3 \cdot 3H_2O$, $RhCl_3 \cdot 3H_2O$, tetra-*n*-butylammonium hexafluorophosphate (TBAP), α-cyano-4-hydroxycinnamic acid, and 4,7,10-trioxa-1,13-tridecanediamine were supplied by Aldrich. Avidin and BSA were obtained from Calbiochem. PD-10 size-exclusion columns and YM-30 centricons were received from GE Healthcare and Millipore, respectively. Autoclaved Milli-Q water was used for the preparation for the aqueous solutions. 4′-Succinimidylcarboxy-4′-methyl-2,2′-bipyridine (bpy-NHS),[32] biotinyl-*N*-hydroxysuccinimidyl ester (biotin-NHS),[2b] *N*-biotinyl-1,6-diaminohexane,[33] bpy-Et,[30f,34] bpy-C6-biotin,[30c] the dimers $[Ir_2(pba)_4Cl_2]$[7a] and $[Rh_2(pba)_4Cl_2]$,[7b] and $[Ir(pba)_2(bpy\text{-}C6\text{-}biotin)](PF_6)$ (**1**)[30h] were synthesized according to literature procedures. Prestained precision protein standards were obtained from Bio-Rad Laboratories. HeLa cells were obtained from the American Type Culture Collection. Dulbecco's modified Eagle's medium (DMEM), fetal bovine serum (FBS), phosphate-buffered saline, trypsin-EDTA, and penicillin/streptomycin were purchased from Invitrogen. The growth medium for cell culture contained DMEM with 10% FBS and 1% penicillin/streptomycin. Alexa Fluor 633-labeled transferrin was obtained from Molecular Probes.

***N*-Boc-4,7,10-trioxa-1,13-tridecanediamine (H_2N-TEG-NHBoc).** A 4,7,10-trioxa-1,13-tridecanediamine solution (6 g, 27.4 mmol) in tetrahydrofuran (THF; 25 mL) was cooled at 0 °C. Di-*tert*-butyl dicarbonate (990 mg, 4.5 mmol) dissolved in THF (10 mL) was added slowly to the solution over 5 min. The resulting mixture was stirred under an inert atmosphere of nitrogen at 0 °C for 2 h. The reaction was allowed to proceed at room temperature for 12 h. The pale-yellow solution was evaporated under vacuum to give a pale-yellow oil, which was purified by chromatography on silica gel. The desired product was eluted using CH_2Cl_2/MeOH (10:1, v/v). Removal of the solvent gave a yellow oil. Yield: 800 mg (55%). Positive-ion electrospray ionization mass spectrometry (ESI-MS) ion clusters were present at *m*/*z* 321 $\{M + H^+\}^+$.

4-[(13-Amino-4,7,10-trioxa)tridecylaminocarbonyl]-4′-methyl-2,2′-bipyridine (bpy-TEG-NH_2). A mixture of H_2N-TEG-NHBoc (436 mg, 1.36 mmol), bpy-NHS (422 mg, 1.36 mmol), and triethylamine (0.3 mL) in *N*,*N*-dimethylformamide (DMF; 30 mL) was stirred under an inert atmosphere of nitrogen at room temperature for 12 h. The pink solution was evaporated under vacuum to give a pink oil. The oil was purified by column chromatography on silica gel. The desired product was eluted using CH_2Cl_2/MeOH (15:1, v/v). Upon removal of the solvent, trifluoroacetic acid (2 mL) was added to the residual pink oil, and the solution was stirred at room temperature for 2 h. The product was dried under vacuum to give a pink oil. Yield: 369 mg (65%). Positive-ion ESI-MS ion clusters were present at *m*/*z* 417 $\{M + H^+\}^+$.

4-[(13-Biotinamido-4,7,10-trioxa)tridecylaminocarbonyl]-4′-methyl-2,2′-bipyridine (bpy-TEG-biotin). A mixture of bpy-TEG-NH_2 (360 mg, 0.86 mmol), biotin-NHS (267 mg, 0.86 mmol), and triethylamine (0.3 mL) in DMF (30 mL) was stirred under nitrogen at room temperature for 12 h. The solvent was removed under vacuum to give a pink oil. The product was purified by column chromatography on silica gel. The desired product was eluted using CH_2Cl_2/MeOH (5:1, v/v). The product was dried under vacuum to give a pink oil. Yield: 332 mg (60%). ^{1}H NMR (300 MHz, methanol-d_4, 298 K, TMS): δ 8.77 (d, 1H, J = 3.6 Hz, H6 of bpy), 8.67 (s, 1H, H3 of bpy), 8.52 (d, 1H, J = 3.6 Hz, H5 of bpy), 8.20 (s, 1H, H3′ of bpy), 7.77 (d, 1H, J = 4.5 Hz, H6′ of bpy), 7.30 (d, 1H, J = 4.2 Hz, H5′ of bpy), 4.49−4.45 (m, 1H, NCH of biotin), 4.29−4.25 (m, 1H, NCH of biotin), 3.65−3.44 (m, 16H, $CH_2CH_2CH_2O(CH_2)_2O(CH_2)_2OCH_2CH_2CH_2$), 2.92−2.86 (m, 1H, SCH of biotin), 2.70−2.66 (m, 2H, SCH of biotin), 2.46 (s, 3H, CH_3 on C4′ of bpy), 2.16 (t, 2H, J = 7.5 Hz, $COCH_2C_3H_6$ of biotin), 1.93−1.89 (m, 2H, bpy-4-$CONHCH_2CH_2$), 1.74−1.33 (m, 8H, CH_2CH_2NH-biotin and $COCH_2C_3H_6$ of biotin). Positive-ion ESI-MS ion clusters were present at *m*/*z* 643 $\{M + H^+\}^+$.

$[Ir(pba)_2(bpy\text{-}TEG\text{-}biotin)](PF_6)$ (2). A mixture of $[Ir_2(pba)_4Cl_2]$ (118 mg, 0.10 mmol) and bpy-TEG-biotin (129 mg, 0.20 mmol) in CH_2Cl_2/MeOH (1:1, v/v; 50 mL) was refluxed under an inert atmosphere of nitrogen in the dark for 12 h. The orange-red solution was then cooled to room temperature, and KPF_6 (147 mg, 0.80 mmol) was added to the solution. The mixture was stirred for 10 min and then evaporated to dryness. The product was purified by column chromatography on silica gel. The desired product was eluted with

(29) Kwon, T.-H.; Kwon, J.; Hong, J.-I. *J. Am. Chem. Soc.* **2008**, *130*, 3726–3727.
(30) (a) Lo, K. K.-W.; Chung, C.-K.; Lee, T. K.-M.; Lui, L.-H.; Tsang, K. H.-K.; Zhu, N. *Inorg. Chem.* **2003**, *42*, 6886–6897. (b) Lo, K. K.-W.; Chan, J. S.-W.; Lui, L.-H.; Chung, C.-K. *Organometallics* **2004**, *23*, 3108–3116. (c) Lo, K. K.-W.; Li, C.-K.; Lau, J. S.-Y. *Organometallics* **2005**, *24*, 4594–4601. (d) Lo, K. K.-W.; Lau, J. S.-Y. *Inorg. Chem.* **2007**, *46*, 700–709. (e) Lo, K. K.-W.; Zhang, K. Y.; Leung, S.-K.; Tang, M.-C. *Angew. Chem., Int. Ed.* **2008**, *47*, 2213–2216. (f) Lo, K. K.-W.; Lee, P.-K.; Lau, J. S.-Y. *Organometallics* **2008**, *27*, 2998–3006. (g) Lau, J. S.-Y.; Lee, P.-K.; Tsang, K. H.-K.; Ng, C. H.-C.; Lam, Y.-W.; Cheng, S.-H.; Lo, K. K.-W. *Inorg. Chem.* **2009**, *48*, 708–718. (h) Zhang, K. Y.; Lo, K. K.-W. *Inorg. Chem.* **2009**, *48*, 6011–6025. (i) Zhang, K. Y.; Li, S. P.-Y.; Zhu, N.; Or, I. W.-S.; Cheung, M. S.-H.; Lam, Y.-W.; Lo, K. K.-W. *Inorg. Chem.* **2010**, *49*, 2530–2540. (j) Li, S. P.-Y.; Liu, H.-W.; Zhang, K. Y.; Lo, K. K.-W. *Chem.—Eur. J.* in press.
(31) Perrin, D. D.; Armarego, W. L. F. *Purification of Laboratory Chemicals*; Pergamon: Oxford, U.K., 1997.
(32) Peek, B. M.; Ross, G. T.; Edwards, S. W.; Meyer, G. J.; Meyer, T. J.; Erickson, B. W. *Int. J. Pept. Protein Res.* **1991**, *38*, 114–123.
(33) Sabatino, G.; Chinol, M.; Paganelli, G.; Papi, S.; Chelli, M.; Leone, G.; Papini, A. M.; De Luca, A.; Ginanneschi, M. *J. Med. Chem.* **2003**, *46*, 3170–3173.
(34) Lo, K. K.-W.; Lee, T. K.-M.; Zhang, K. Y. *Inorg. Chim. Acta* **2006**, *359*, 1845–1854.

CH_2Cl_2/MeOH (4:1, v/v). Subsequent recrystallization from CH_2Cl_2/diethyl ether afforded complex **2** as an orange solid. Yield: 175 mg (65%). ^{1}H NMR (300 MHz, acetone-d_6, 298 K, TMS): δ 9.76 (s, 2H, CHO), 9.18 (s, 1H, H3 of bpy), 8.92 (s, 1H, H3′ of bpy), 8.58−8.56 (m, 1H, bpy-4-CONH), 8.44 (d, 2H, J = 8.4 Hz, H3 of the phenyl ring of pba), 8.24−7.97 (m, 10H, H5, H5′, H6, and H6′ of bpy and H3, H4, and H6 of the pyridyl ring of pba), 7.61−7.52 (m, 2H, H6 of the phenyl ring of pba), 7.35−7.31 (m, 2H, H5 of the pyridyl ring of pba), 7.21−7.19 (m, 1H, TEG-NHCO-biotin), 6.87 (dd, 2H, J = 9.4 and 1.6 Hz, H4 of the phenyl ring of pba), 6.26 (s, 1H, NH of biotin), 5.98 (s, 1H, NH of biotin), 4.52−4.50 (m, 1H, NCH of biotin), 4.35−4.32 (m, 1H, NCH of biotin), 3.60−3.40 (m, 16H, $CH_2CH_2CH_2O(CH_2)_2O(CH_2)_2OCH_2CH_2CH_2$), 2.95−2.87 (m, 1H, SCH of biotin), 2.72−2.67 (m, 2H, SCH of biotin), 2.64 (s, 3H, CH_3 on C4′ of bpy), 2.12 (t, 2H, J = 3.2 Hz, $COCH_2C_3H_6$ of biotin), 1.89−1.86 (m, 2H, bpy-4-$CONHCH_2CH_2$), 1.78−1.54 (m, 8H, CH_2CH_2NH-biotin and $COCH_2C_3H_6$ of biotin). Anal. Calcd for $C_{56}H_{62}F_6IrN_8O_8PS\cdot 1.5CH_3OH$: C, 49.60; H, 4.92, N, 8.05. Found: C, 49.52; H, 5.13; N, 7.82. IR (KBr) ν/cm^{-1}: 3432 (br s, NH), 1686 (s, C═O), 845 (s, PF_6^-). Positive-ion ESI-MS ion clusters were present at m/z 1199 $\{M^+\}^+$.

[Rh(pba)$_2$(bpy-C6-biotin)](PF$_6$) (3). The synthetic procedure was similar to that of complex **2**, except that $[Rh_2(pba)_4Cl_2]$ (101 mg, 0.10 mmol) and bpy-C6-biotin (108 mg, 0.20 mmol) were used instead of $[Ir_2(pba)_4Cl_2]$ and bpy-TEG-biotin. Subsequent recrystallization from CH_2Cl_2/diethyl ether afforded complex **3** as a yellow solid. Yield: 120 mg (52%). ^{1}H NMR (300 MHz, acetone-d_6, 298 K, TMS): δ 9.76 (s, 2H, CHO), 9.25−9.21 (m, 2H, bpy-4-CONH and H3 of bpy), 8.86 (s, 1H, H3′ of bpy), 8.46 (d, 2H, J = 6.9 Hz, H3 of the phenyl ring of pba), 8.24−8.18 (m, 5H, H6 of bpy and H3 and H4 of the pyridyl ring of pba), 8.06−7.98 (m, 6H, H5, H5′, and H6′ of bpy, NHCOC$_4$H$_8$ of biotin, and H6 of the pyridyl ring of pba), 7.66 (d, 2H, J = 7.2 Hz, H4 of the phenyl ring of pba), 7.40−7.37 (m, 2H, H5 of the pyridyl ring of pba), 6.87 (d, 2H, J = 5.1 Hz, H6 of the phenyl ring of pba), 5.10 (s, 1H, NH of biotin), 4.89 (s, 1H, NH of biotin), 4.61−4.43 (m, 1H, NCH of biotin), 4.33−4.23 (m, 1H, NCH of biotin), 3.48−3.39 (m, 2H, bpy-4-$CONHCH_2$), 3.20−3.10 (m, 3H, SCH and CH_2NHCOC$_4$H$_8$ of biotin), 2.98 (s, 1H, SCH of biotin), 2.70 − 2.54 (m, 4H, SCH of biotin and CH_3 on C4′ of bpy), 1.84−1.83 (m, 2H, NHCOCH_2C$_3$H$_6$ of biotin), 1.69−1.42 (m, 14H, NHCH_2C$_4$H$_8$-CH_2NH and $COCH_2C_3H_6$ of biotin). Anal. Calcd for $C_{52}H_{54}F_6N_8O_5PRhS\cdot CH_2Cl_2$: C, 51.50; H, 4.57, N, 9.07. Found: C, 51.21; H, 4.29; N, 8.97. IR (KBr) ν/cm^{-1}: 3423 (br s, NH), 1686 (s, C═O), 846 (s, PF_6^-). Positive-ion ESI-MS ion clusters were present at m/z 1006 $\{M^+\}^+$.

[Ir(pba)$_2$(bpy-Et)](PF$_6$) (4). The synthetic procedure was similar to that of complex **2** except that bpy-Et (48 mg, 0.20 mmol) was used instead of bpy-TEG-biotin. Subsequent recrystallization from CH_2Cl_2/diethyl ether afforded complex **4** as an orange solid. Yield: 123 mg (64%). ^{1}H NMR (300 MHz, acetone-d_6, 298 K, TMS): δ 9.75 (s, 2H, CHO), 9.19 (s, 1H, H3 of bpy), 8.93 (s, 1H, H3′ of bpy), 8.42 (d, 2H, J = 7.8 Hz, H3 of the phenyl ring of pba), 8.43−8.07 (m, 5H, H6 of bpy and H5 and H6 of the pyridyl ring of pba), 8.04−7.83 (m, 5H, H5 and H6′ of bpy, bpy-4-CONH, and H3 of the pyridyl ring of pba), 7.58−7.52 (m, 3H, H5′ of bpy and H4 of the phenyl ring of pba), 7.21−7.08 (m, 2H, H4 of the pyridyl ring of pba), 6.87 (d, 2H, J = 3.3 Hz, H6 of the phenyl ring of pba), 3.46−3.41 (m, 2H, bpy-4-$CONHCH_2$), 2.62 (s, 3H, CH_3 on C4′ of bpy), 1.18 (t, 3H, J = 7.5 Hz, bpy-4-$CONHCH_2CH_3$). Anal. Calcd for $C_{38}H_{31}F_6IrN_5O_3P\cdot 2CH_3OH$: C, 47.71; H, 3.90; N, 6.94. Found: C, 47.93; H, 3.78; N, 6.71. IR (KBr) ν/cm^{-1}: 3440 (br s, NH), 1686 (s, C═O), 845 (s, PF_6^-). Positive-ion ESI-MS ion clusters were present at m/z 798 $\{M^+\}^+$.

[Rh(pba)$_2$(bpy-Et)](PF$_6$) (5). The synthetic procedure was similar to that of complex **3**, except that bpy-Et (48 mg, 0.20 mmol) was used instead of bpy-C6-biotin. Subsequent recrystallization from CH_2Cl_2/diethyl ether afforded complex **5** as a yellow solid. Yield: 92 mg (54%). ^{1}H NMR (300 MHz, acetone-d_6, 298 K, TMS): δ 9.75 (s, 2H, CHO), 9.09 (s, 1H, H3 of bpy), 8.84 (s, 1H, H3′ of bpy), 8.43 (d, 2H, J = 9.6 Hz, H3 of the phenyl ring of pba), 8.26−8.08 (m, 5H, H6 of bpy and H3 and H4 of the pyridyl ring of pba), 8.00−7.92 (m, 5H, H5 and H6′ of bpy, bpy-4-CONH, and H6 of the pyridyl ring of pba), 7.67−7.61 (m, 3H, H5′ of bpy and H4 of the phenyl ring of pba), 7.39−7.36 (m, 2H, H5 of the pyridyl ring of pba), 6.68 (d, 2H, J = 4.2 Hz, H6 of the phenyl ring of pba), 3.44 (q, 2H, J = 1.5 Hz, bpy-4-$CONHCH_2$), 2.59 (s, 3H, CH_3 of C4′ of bpy), 1.17 (t, 3H, J = 5.1 Hz, bpy-4-$CONHCH_2CH_3$). Anal. Calcd for $C_{38}H_{31}F_6N_5O_3PRh\cdot 1.5CH_3OH$: C, 52.62; H, 4.14; N, 7.77. Found: C, 52.42; H, 4.13; N, 7.49. IR (KBr) ν/cm^{-1}: 3441 (br s, NH), 1685 (s, C═O), 845 (s, PF_6^-). Positive-ion ESI-MS ion clusters were present at m/z 709 $\{M^+\}^+$.

[Ir(ppy-CH$_2$NHC$_4$H$_9$)$_2$(bpy-TEG-biotin)](PF$_6$) (2a). A mixture of complex **2** (135 mg, 0.10 mmol), *n*-butylamine (68 mg, 0.20 mmol), and triethylamine (0.5 mL) in MeOH (40 mL) was refluxed under an inert atmosphere of nitrogen in the dark for 12 h. After the orange solution was cooled to room temperature, solid $NaBH_4$ (34 mg, 0.88 mmol) was added to the solution. The solution was then stirred under an inert atmosphere of nitrogen for 4 h and then evaporated to dryness. The orange solid was redissolved in CH_2Cl_2 (50 mL), and the solution was washed with distilled water (30 mL × 3). The CH_2Cl_2 layer was then dried over anhydrous $MgSO_4$, filtered, and evaporated to dryness to give an orange solid. Subsequent recrystallization of the product from a CH_2Cl_2/diethyl ether mixture afforded complex **2a** as an orange solid. Yield: 90 mg (62%). ^{1}H NMR (300 MHz, methanol-d_4, 298 K, TMS): δ 9.03 (s, 1H, H3 of bpy), 8.67 (s, 1H, H3′ of bpy), 8.14−8.12 (m, 3H, H6 of bpy and H3 of the pyridyl ring of ppy), 7.89−7.81 (m, 6H, H5 and H6′ of bpy, H3 of the phenyl ring of ppy, and H4 of the pyridyl ring of ppy), 7.65−7.61 (m, 2H, H6 of the pyridyl ring of ppy), 7.42 (d, 1H, J = 5.7 Hz, H5′ of bpy), 7.08−7.03 (m, 4H, H4 of the phenyl ring of ppy and H5 of the pyridyl ring of ppy), 6.25 (d, 2H, J = 9.0 Hz, H6 of the phenyl ring of ppy), 4.49−4.45 (m, 1H, NCH of biotin), 4.30−4.26 (m, 1H, NCH of biotin), 3.61−3.41 (m, 16H, $CH_2CH_2CH_2O(CH_2)_2O(CH_2)_2OCH_2CH_2CH_2$), 3.24−3.14 (m, 4H, ppy-CH_2), 2.93−2.87 (m, 1H, SCH of biotin), 2.69−2.65 (m, 2H, SCH of biotin), 2.61 (s, 3H, CH_3 on C4′ of bpy), 2.40 (t, 4H, J = 7.2 Hz, ppy-CH_2NHCH_2), 2.16 (t, 2H, J = 7.2 Hz, $COCH_2C_3H_6$ of biotin), 1.90−1.71 (m, 2H, bpy-4-$CONHCH_2CH_2$), 1.71−1.53 (m, 6H, CH_2CH_2NH-biotin and ppy-CH_2NHCH_2CH_2), 1.43−1.30 (m, 6H, NHCOCH_2C$_3$H$_6$ of biotin), 1.25−1.20 (m, 4H, ppy-CH_2NH$(CH_2)_2CH_2$), 0.88 (t, 6H, J = 7.2 Hz, ppy-CH_2NH$(CH_2)_3CH_3$). Anal. Calcd for $C_{64}H_{84}F_6IrN_{10}O_6PS\cdot 0.5(C_2H_5)_2O$: C, 53.00; H, 6.00, N, 9.36. Found: C, 52.82; H, 6.29; N, 9.51. IR (KBr) ν/cm^{-1}: 3423 (br s, NH), 1686 (s, C═O), 846 (s, PF_6^-). Positive-ion ESI-MS ion clusters were present at m/z 1314 $\{M^+\}^+$.

Physical Measurements, Instrumentation, and Methods. The instruments for characterization and photophysical and electrochemical studies were described previously.[30h] The methods by which determination of the luminescence quantum yields,[35,36] HABA assays,[30h] emission titrations,[30e] MTT assays,[38] and live-cell confocal imaging[30h] were undertaken were also reported previously.

Biotinylation of BSA. The iridium(III) or rhodium(III) complex (0.65 μmol) in anhydrous dimethyl sulfoxide (DMSO; 50 μL) was added to a solution of BSA (5 mg, 76 nmol) in a 50 mM carbonate buffer at pH 9.0 (500 μL). After the suspension was stirred in the dark at room temperature for 12 h, Na(CN)BH_3 (20 mg, 317 μmol) in NaOH (2 M, 20 μL) was added to the solution. The solution was stirred in the dark at room temperature for 12 h. The solid residue was removed by centrifugation.

(35) Demas, J. N.; Crosby, G. A. *J. Phys. Chem.* **1971**, *75*, 991–1024.
(36) Nakamura, K. *Bull. Chem. Soc. Jpn.* **1982**, *55*, 2697–2705.

Table 1. Electronic Absorption Spectral Data of the Iridium(III) and Rhodium(III) Complexes at 298 K

complex	solvent	λ_{abs}/nm (ε/dm^3 mol^{-1} cm^{-1})
1	CH_2Cl_2	259 sh (49 115), 272 (51 835), 295 sh (39 150), 318 sh (29 810), 364 sh (8585), 411 sh (4410)
	CH_3CN	259 sh (59 785), 268 (61 290), 300 sh (43 885), 318 sh (33 520), 369 sh (8965), 416 (4850)
2	CH_2Cl_2	249 sh (37 260), 274 (50 365), 300 (40 725), 320 sh (31 685), 373 sh (6745), 422 sh (4415), 449 (3625)
	CH_3CN	246 sh (36 775), 271 (49 780), 299 (39 495), 320 sh (28 580), 370 sh (6780), 421 sh (4245), 445 (3445)
2a	CH_2Cl_2	260 (48 845), 272 sh (47 235), 320 sh (21 510), 355 sh (9090), 383 sh (7220), 416 sh (3990)
	CH_3CN	258 (43 670), 273 sh (41 615), 315 sh (20 335), 358 sh (7905), 381 sh (6595), 413 sh (3640)
3	CH_2Cl_2	251 sh (41 640), 268 (42 300), 304 (38 285), 312 sh (37 490), 331 sh (19 305), 394 (6075), 415 sh (2420)
	CH_3CN	249 sh (43 250), 268 (44 665), 301 (38 790), 311 sh (37 850), 331 sh (18 250), 389 (7065), 414 sh (1680)
4	CH_2Cl_2	256 sh (48 950), 271 (50 940), 292 sh (37 955), 318 sh (25 930), 357 sh (9030), 410 (4235)
	CH_3CN	252 sh (45 810), 269 (47 825), 292 sh (33 680), 315 sh (24 730), 360 sh (7640), 412 (3520)
5	CH_2Cl_2	249 (57 630), 271 (58 095), 303 (57 235), 312 sh (55 530), 328 sh (34 380), 396 (8985), 420 sh (3795)
	CH_3CN	242 (35 565), 268 (36 820), 298 (35 750), 309 sh (34 805), 324 sh (24 630), 386 (6530), 414 sh (1665)

The supernatant was then loaded onto a PD-10 column that had been equilibrated with a 50 mM potassium phosphate buffer at pH 7.4. The first orange-yellow band was collected. The solution was then concentrated with a YM-30 centricon, washed successively with a potassium phosphate buffer, and stored at 4 °C before use.

Sodium Dodecyl Sulfate Polyacrylamide Gel Electrophoresis (SDS-PAGE) of Bioconjugates 1-BSA−5-BSA. The bioconjugate sample ([BSA] = ca. 100 μM, 10 μL) was mixed with a sample buffer (25% glycerol, 5% β-mercaptoethanol, 2% SDS, and 0.01% bromophenol blue in 0.06 M Tris-HCl at pH 6.8; 20 μL). The mixture was denatured at 95 °C for 5 min before being loaded into 8% polyacrylamide gel for SDS-PAGE analysis using Bio-Rad electrophoresis accessories.[39a] The gel was directly analyzed using a Fujifilm LAS-4000 luminescent image analyzer before and after staining with Coomassie blue.

Results and Discussion

Complex Design and Synthesis. Each of the luminescent biotinylation reagents, complexes **1**−**3**, contained one biotin-modified diimine ligand and two pba ligands. A C6 or triethylene glycol (TEG) spacer arm has been introduced to the complexes to investigate the effects of hydrophilicity and the chain length of the spacer arm on the avidin-binding properties of the resultant bioconjugates. The pba ligand was used in view of its facile reaction with the primary amine groups of biomolecules.[7] The bis(pyridylbenzaldehyde) complexes **1**−**5** were obtained from the reaction of the precursor complex [M_2(pba)$_4$Cl$_2$] (M = Ir, Rh) and the diimine ligand (bpy-C6-biotin, bpy-TEG-biotin, and bpy-Et) in refluxing CH_2Cl_2/MeOH, followed by anion exchange with KPF_6. They were purified by column chromatography on silica gel and recrystallization. To examine the reactivity of aldehyde groups, complex **2** was reacted with a model substrate *n*-butylamine, resulting in the formation of complex **2a**. All of the complexes have been characterized by ^{1}H NMR spectroscopy, positive-ion ESI-MS, IR spectroscopy, and microanalysis.

Electronic Absorption Spectroscopy. The electronic absorption spectral data of the cyclometalated iridium(III) and rhodium(III) polypyridine complexes in CH_2Cl_2 and CH_3CN at 298 K are listed in Table 1. The electronic absorption spectra of complexes **4** and **5** in CH_2Cl_2 at 298 K are shown in Figure 1 as examples. The electronic absorption spectra of all of the complexes showed intense spin-allowed intraligand (^{1}IL) ($\pi \rightarrow \pi^*$) (N^N and N^C) absorption bands and shoulders at ca. 242−350 nm (ε on the order of 10^4 dm^3 mol^{-1} cm^{-1}) and less intense spin-allowed metal-to-ligand charge-transfer (^{1}MLCT) [dπ(Ir or Rh) → π^*(N^N and N^C)] shoulders at ca. 350−450 nm.[7,8a,d,9,11,12a,13,14,15a,c,16−23,24b−d,25−27,29,30a−d,f−j]

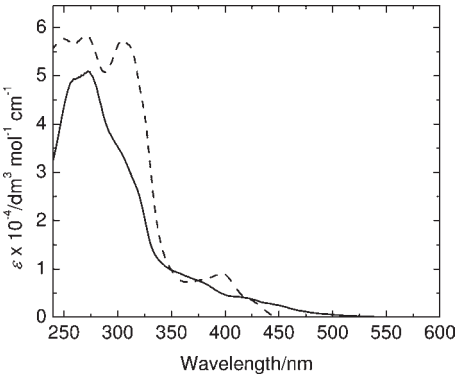

Figure 1. Electronic absorption spectra of complexes **4** (solid line) and **5** (dashed line) in CH_2Cl_2 at 298 K.

In addition, weaker absorption tails toward the lower energy region were observed at > 450 nm for all of the iridium(III) complexes, which can be attributed to spin-forbidden ^{3}MLCT [dπ(Ir) → π^*(N^N and N^C)] transitions.[7−9,11,12c,13b,14,15a,c,16−23,24b−d,25−27,30a−d,f−j] In general, the low-energy (LE) absorption features of the rhodium(III) complexes are higher in energy compared to the iridium(III) analogues, probably because of the lower dπ orbital energy of the rhodium(III) center, which is in agreement with the assignment of MLCT transitions. Another possible reason is the negligible singlet−triplet absorption as a result of the much weaker spin−orbital coupling for the rhodium(III) complexes.

Luminescence Properties. The photophysical data of all of the complexes are summarized in Table 2. The iridium(III) bis(pyridylbenzaldehyde) complexes **1**, **2**, and **4** exhibited intense and long-lived orange-yellow luminescence upon irradiation in fluid solutions under ambient conditions and in alcohol glass at 77 K. These iridium(III) complexes shared similar photophysical properties; for example, they showed structured emission spectral profiles and very long emission lifetimes (2.20−3.90 μs) in fluid solutions at 298 K. The emission spectra of complex **2** in degassed CH_2Cl_2 and CH_3CN at 298 K and in alcohol glass at 77 K are shown in Figure 2. The emission maxima of these iridium(III) complexes were insensitive toward the polarity of the solvents. Upon cooling to 77 K, only small blue shifts of the emission maxima were observed. These findings suggest that the emission is derived from a ^{3}IL ($\pi \rightarrow \pi^*$) (pba) excited state, probably with mixing of some ^{3}MLCT [dπ(Ir) → π^*(pba)] character.[7a,c,30j]

Table 2. Photophysical Data of the Iridium(III) and Rhodium(III) Complexes[a]

complex	medium (T/K)	λ_{em}/nm	τ_o/μs	Φ_{em}
1	CH_2Cl_2 (298)	539 (max), 568	2.89	0.37
	CH_3CN (298)	540 (max), 570	2.98	0.21
	glass[b] (77)	529 (max), 567, 606 sh	6.02	
2	CH_2Cl_2 (298)	535, 570 sh	3.90	0.48
	CH_3CN (298)	536, 570 sh	2.95	0.31
	glass[b] (77)	523 (max), 564, 615 sh	6.74	
2a	CH_2Cl_2 (298)	500, 532 sh, 584 (max)	1.65 0.39	0.11
	CH_3CN (298)	491 (max), 521 sh, 607	1.74 0.14	0.08
	MeOH (298)	493 (max), 520, 602 sh	1.93 0.086	0.044
	buffer[c] (298)	490 (max), 518	2.93	0.017
	glass[b] (77)	482, 525 (max), 570 sh	5.36	
3	CH_2Cl_2 (298)	509 (max), 546, 586 sh	2.89	0.010
	CH_3CN (298)	509 (max), 546, 583 sh	5.91	0.008
	glass[b] (77)	504 (max), 543, 573 sh	161.56	
4	CH_2Cl_2 (298)	539 sh, 570	2.20	0.34
	CH_3CN (298)	543, 571 (max)	2.67	0.24
	glass[b] (77)	527 (max), 564, 592 sh	5.12	
5	CH_2Cl_2 (298)	509 (max), 546, 586 sh	3.97	0.014
	CH_3CN (298)	510, 543 (max), 583 sh	3.86	0.017
	glass[b] (77)	507 (max), 547, 588 sh	175.65	

[a] Excitation wavelength = 350 nm. [b] EtOH/MeOH (4:1, v/v). [c] 50 mM potassium phosphate buffer at pH 7.4/DMSO (95:5, v/v).

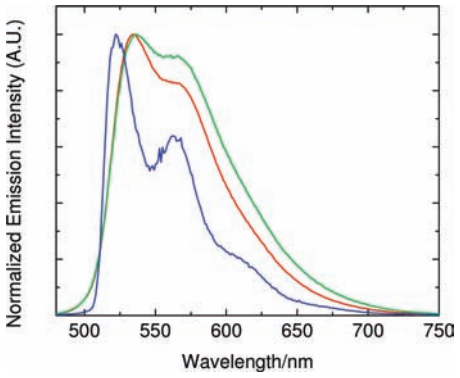

Figure 2. Emission spectra of complex **2** in CH_2Cl_2 (red) and CH_3CN (green) at 298 K and in EtOH/MeOH (4:1, v/v) at 77 K (blue).

Photoexcitation of the rhodium(III) complexes **3** and **5** resulted in comparatively weak greenish-yellow emission in solutions at room temperature but intense and exceptionally long-lived (τ_o = 162−176 μs) greenish-yellow emission in low-temperature glass. The emission spectra of complex **3** in degassed CH_2Cl_2 and CH_3CN at 298 K and in alcohol glass at 77 K are illustrated in Figure 3. Compared to the iridium(III) aldehyde complexes, the rhodium(III) complexes displayed more structured emission bands at shorter wavelengths and the emission energy was also insensitive to solvent polarity. It is likely that the emission originates from a ^{3}IL ($\pi \rightarrow \pi^*$) (pba) excited state, probably with mixing of some ^{3}MLCT [dπ(Rh) $\rightarrow \pi^*$(pba)] character,[7b,8d,9,11,12c] which is in line with the lower dπ orbital energy of the rhodium(III) center and the observation of higher emission energy for the rhodium(III) complexes.

It is interesting to note that complex **2a** exhibited dual-emissive properties in fluid solutions at room temperature upon photoexcitation (Table 2). As shown in Figure 4, this complex displayed highly environmentally sensitive emission profiles. In a degassed polar aqueous buffer, a

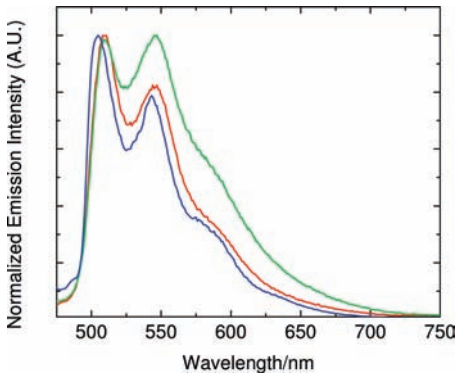

Figure 3. Emission spectra of complex **3** in CH_2Cl_2 (red) and CH_3CN (green) at 298 K and in EtOH/MeOH (4:1, v/v) at 77 K (blue).

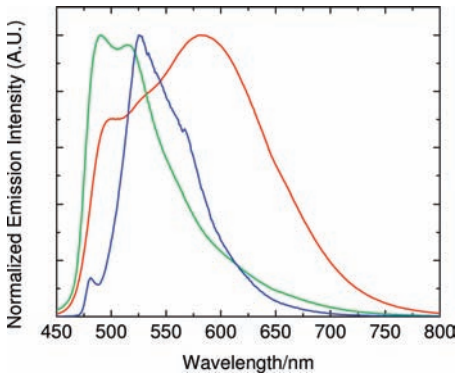

Figure 4. Emission spectra of complex **2a** in CH_2Cl_2 (red) and a 50 mM potassium phosphate buffer at pH 7.4/DMSO (95:5, v/v) (green) at 298 K and in EtOH/MeOH (4:1, v/v) at 77 K (blue).

high-energy (HE) emission band with structural features at ca. 490−520 nm was shown. However, an additional LE broad band appeared at ca. 584 nm in relatively nonpolar CH_2Cl_2 (Table 2 and Figure 4). With reference to our previous photophysical studies on related dual-emissive cyclometalated iridium(III) diimine systems,[30e] the HE emission has been tentatively assigned to a ^{3}IL ($\pi \rightarrow \pi^*$) (N^N and N^C) excited state, while the emissive state of the LE emission should possess high triplet charge-transfer character. In rigid glass at 77 K, complex **2a** exhibited intense and long-lived greenish-yellow emission with a vibronically structured band, which suggests that the emission originates from a ^{3}IL/^{3}MLCT state.[30e]

Electrochemical Properties. The electrochemical properties of all of the complexes have been studied by cyclic voltammetry. The electrochemical data are listed in Table 3. The iridium(III) complexes **1**, **2**, **2a**, and **4** exhibited an irreversible wave at ca. +1.53 to +1.37 V versus saturated calomel electrode (SCE), while the rhodium(III) complexes **3** and **5** displayed an irreversible oxidation wave at ca. +1.52 and +1.63 V, respectively. These irreversible waves have been assigned to the metal-centered M(IV/III) oxidation processes.[7,8c,d,9a,b,11a,b,14a,b,15a,16,17b,18a,b,19d,20,21b,d,22,26,27,30a−d,f−i] Irreversible metal-centered oxidation waves have been observed in cyclometalated iridium(III) and rhodium(III) systems, especially where the highest occupied molecular orbitals are associated with metal−ligand character or the oxidation of ligands.[9b,14a,16b] Complex **2a** revealed an additional irreversible wave at ca. 1.07 V, attributable to the oxidation of the secondary amines of the cyclometalating

Table 3. Electrochemical Data of the Iridium(III) and Rhodium(III) Complexes[a]

complex	oxidation, E_a/V	reduction, $E_{1/2}$ or E_c/V
1	+1.51[b]	−1.23, −1.60,[c] −1.74,[b] −2.05,[b] −2.30[b]
2	+1.48[b]	−1.26, −1.59,[c] −1.77,[b] −2.19,[b] −2.31[b]
2a	+1.07,[b] +1.37[b]	−1.30, −1.83,[c] −2.27,[b] −2.50,[b] −2.70[b]
3	+1.52[b]	−1.31, −1.69,[c] −2.04,[b] −2.21[b], −2.33[b]
4	+1.53[b]	−1.26, −1.62,[c] −1.90,[b] −2.20[b]
5	+1.63[b]	−1.33, −1.67,[b] −2.39[b]

[a] In CH_3CN (0.1 M TBAP) at 298 K (glassy carbon working electrode, sweep rate = 100 mV s^{-1}, all potentials versus SCE). [b] Irreversible waves. [c] Quasi-reversible couples.

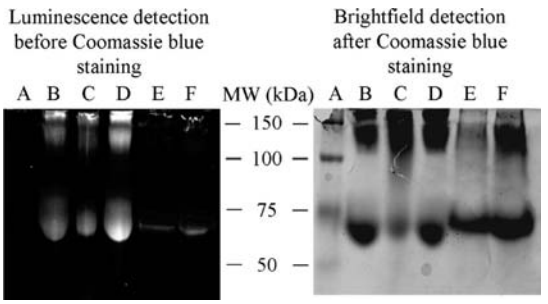

Figure 5. SDS-PAGE analysis of bioconjugates **1-BSA**−**5-BSA**. Lanes A−F correspond to prestained protein standards, bioconjugates **1-BSA**, **2-BSA**, **4-BSA**, **3-BSA**, and **5-BSA**, respectively.

ligands.[30b,d] In addition, all of the complexes showed a reversible couple at ca. −1.3 V, which has been assigned to the reduction of the diimine ligands.[7,8c,d,9a,b,11a,b,15a,16,17b,18a,b,19d,20,21b,d,22,23a,25a,26,30a−d,f−i] Several quasi-reversible couples or irreversible waves at more negative potentials have also been observed, and they have been ascribed to the reduction of the diimine and cyclometalating ligands.[7,9a,b,11b,16a,c,17b,18b,21b,d,22,23a,30a,d,f−i]

Biotinylation of BSA. After the amine reactivity of the aldehyde groups of complex **2** has been studied, we have biotinylated BSA with all of the aldehyde complexes **1**−**5**. The resultant bioconjugates **1-BSA**−**5-BSA** have been isolated and purified by size-exclusion chromatography and ultrafiltration; evaluation of the purification has been included in the Supporting Information (Figure S1). The luminescent iridium(III) and rhodium(III) bioconjugates have been analyzed by SDS-PAGE before and after Coomassie blue staining (Figure 5). The luminescent bands corresponding to molecular weights of ca. 66 and 132 kDa have been attributed to monomeric and dimeric BSA molecules, respectively. These results indicate the covalent labeling and cross-linking abilities of the luminescent bis(pyridylbenzaldehyde) complexes.[7] Bioconjugate **2-BSA** has also been analyzed by MALDI-TOF MS as an example to further investigate the bioconjugation reaction. Compared to the MS spectrum of unmodified BSA, an increase of ca. 1137 mass units was observed in the MS spectrum of bioconjugate **2-BSA** (Figure S2 in the Supporting Information; m/z 66 408 for BSA and m/z 67 545 for bioconjugate **2-BSA**), attributable to the addition of one complex molecule (MW = 1183).[39b] Nevertheless, the relatively broad peaks in the mass spectrum of bioconjugate **2-BSA** suggest a mixture of BSA molecules modified by various numbers of complex **2**. Additionally, the electronic absorption spectra of the conjugates have been examined. On the basis of the spectral data of the free complexes and their bioconjugates, the dye-to-protein ratios (D/P) of the bioconjugates have been determined to be ca. 0.9−4.5 (Table 4).[39c]

Table 4. Dye-to-Protein Ratios and Photophysical Data of Bioconjugates **1-BSA**−**5-BSA** in a Degassed 50 mM Potassium Phosphate Buffer at pH 7.4 and 298 K[a]

bioconjugate	D/P ratio	λ_{em}/nm	τ_o/μs	Φ_{em}
1-BSA	2.0	574	0.60 (83%), 0.17 (17%)	0.01
2-BSA	0.9	570	1.65 (60%), 0.48 (40%)	0.038
3-BSA	4.5	529 (max), 551	0.95	0.002
4-BSA	1.7	568	1.37 (64%), 0.40 (36%)	0.018
5-BSA	1.6	532, 555 sh	1.76	0.003

[a] Excitation wavelength = 350 nm.

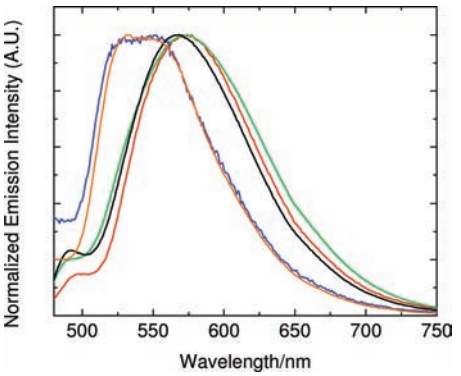

Figure 6. Emission spectra of bioconjugates **1-BSA** (red), **2-BSA** (green), **3-BSA** (blue), **4-BSA** (black), and **5-BSA** (orange) in a 50 mM potassium phosphate buffer at pH 7.4 and 298 K.

Upon photoexcitation at 350 nm, all of the bioconjugates **1-BSA**−**5-BSA** showed moderately intense and long-lived orange-to-yellow emission in a degassed potassium phosphate buffer under ambient conditions (Table 4). The emission spectra are shown in Figure 6. The iridium(III) bioconjugates **1-BSA**, **2-BSA**, and **4-BSA** displayed broad emisison bands at ca. 570 nm. The emission of these bioconjugates showed biexponential decay (Table 4), which is not uncommon for biomolecules labeled with luminescent transition-metal complexes.[6a,7,30a,37] The lifetimes were on the microsecond or submicrosecond time scale, indicative of the phosphorescence nature of the emission. Upon bioconjugation, the aldehyde moieties were converted to the electron-donating secondary amines. It is likely that the emission of the iridium(III) bioconjugates originates from an excited state of predominant ^{3}MLCT [dπ(Ir) → π^*(N^N)] character.[7a,c] Unlike complex **2a**, [Ir(ppy-$CH_2NHC_4H_9$)$_2$(bpy-C6-biotin)](PF_6),[30e] and [Ir(ppy-$CH_2NHC_4H_9$)$_2$(bpy-Et)](PF_6),[30e] no predominant HE band at ca. 490 nm was observed for the iridium(III) bioconjugates in a degassed aqueous buffer. This is probably due to the close proximity of the luminescent cores to the relatively nonpolar protein molecule because the LE emission feature is predominant in a relatively nonpolar

(37) (a) Lo, K. K.-W.; Ng, D. C.-M.; Hui, W.-K.; Cheung, K.-K. *J. Chem. Soc., Dalton Trans.* **2001**, 2634–2640. (b) Lo, K. K.-W.; Hui, W.-K.; Ng, D. C.-M.; Cheung, K.-K. *Inorg. Chem.* **2002**, *41*, 40–46.
(38) Mosmann, T. *J. Immunol. Methods* **1983**, *65*, 55–63.
(39) (a) Laemmli, U. K. *Nature* **1970**, *227*, 680–685. (b) Shi, W.; Dolai, S.; Averick, S.; Fernando, S. S.; Saltos, J. A.; L'Amoreaux, W.; Banerjee, P.; Raja, K. *Bioconjugate Chem.* **2009**, *20*, 1595–1601. (c) Castellano, F. N.; Dattelbaum, J. D.; Lakowicz, J. R. *Anal. Biochem.* **1998**, *255*, 165–170.

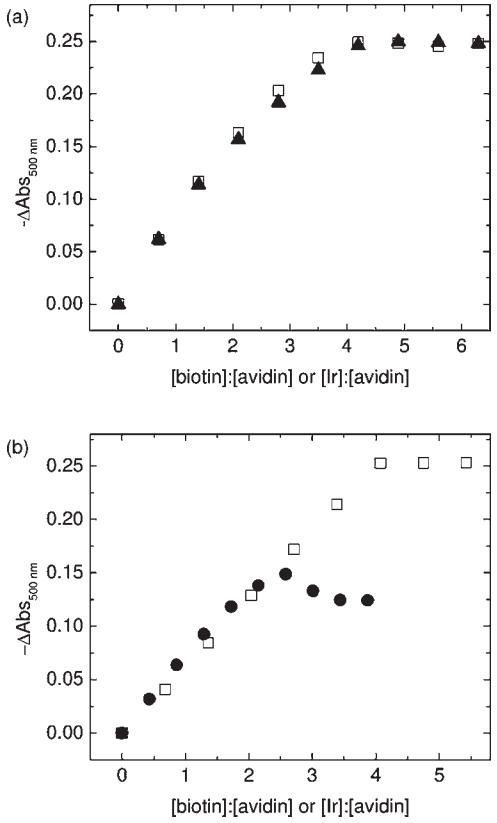

Figure 7. Results of spectrophotometric titrations of avidin-$(HABA)_4$ with (a) complex **2a** (solid triangles) and (b) bioconjugate **2-BSA** (solid circles). The results of titrations with unmodified biotin are included in both figures (open squares).

environment. The rhodium(III) bioconjugates **3-BSA** and **5-BSA** exhibited structured emission bands at ca. 530 and 550 nm (Figure 6). The emissive state probably possesses much ^{3}IL ($\pi \rightarrow \pi^*$) (N^N and N^C) character.[7b] However, the mixing of ^{3}MLCT [dπ(Rh) $\rightarrow$ π^*(N^N)] character cannot be excluded owing to the observation of a higher emission energy for the rhodium(III) bioconjugates compared to their iridium(III) counterparts, which may result from the lower dπ orbital energy of the rhodium(III) center.

HABA Assays. The avidin-binding properties of complexes **1**−**3** and **2a** and bioconjugates **1-BSA**−**3-BSA** have been studied by HABA assays.[1a,4] As an example, the titration results of complex **2a** showed an equivalence point at [Ir]:[avidin] = ca. 4 and $-\Delta Abs_{500\ nm}$ = ca. 0.25, which are indistinguishable from those of unmodified biotin (Figure 7a). Similar spectrophotometric titration curves have also been obtained for complexes **1**−**3** (Figure S3 in the Supporting Information). These observations indicate the specific binding of the biotin moieties of these complexes to avidin. We found that the addition of bioconjugate **2-BSA** to a mixture of HABA and avidin induced a substantial decrease of absorbance at 500 nm (Figure 7b), while the other two biotinylated bioconjugates **1-BSA** and **3-BSA** did not show any significant changes. Because the presence of free BSA did not interfere with the avidin-binding properties of the biotin complexes **1**−**3** (Figure S4 in the Supporting Information), it can be concluded that the absence of spectrophotometric changes for **1-BSA** and **3-BSA** is a consequence of the

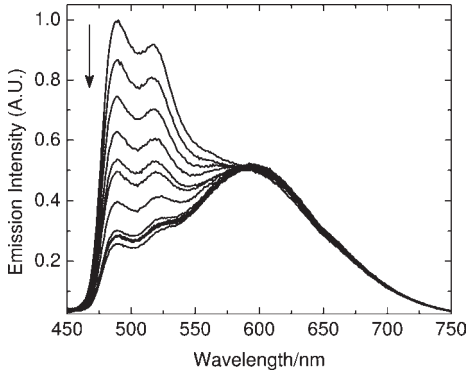

Figure 8. Emission spectral traces of complex **2a** upon the addition of avidin in an aerated 50 mM potassium phosphate buffer at pH 7.4/DMSO (95:5, v/v).

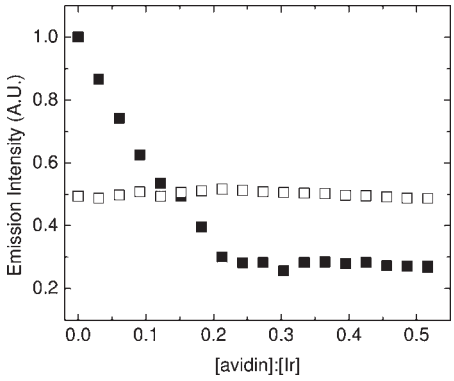

Figure 9. Emission titration curves for the titration of complex **2a** with avidin. The emission intensities were measured at 490 nm (solid squares) and 600 nm (open squares).

Table 5. Cytotoxicity of the Iridium(III) and Rhodium(III) Complexes and Cisplatin toward a HeLa Cell Line after Incubation of Complexes for 48 h

complex	$IC_{50}/\mu M$
1	58.4 ± 5.4
2	61.4 ± 4.4
2a	37.4 ± 5.0
3	57.8 ± 13.6
4	30.5 ± 4.8
5	34.7 ± 5.6
cisplatin	32.6 ± 4.34

steric hindrance associated with the conjugated BSA molecules. It is conceivable that the C6 spacer arm (ca. 13 Å between the two amide carbons) is not sufficiently long for the biotin groups of these BSA conjugates to gain access to the specific binding sites of avidin (ca. 9 Å below the protein surface).[3b] This is in accordance with the result of our previous study on luminescent rhenium(I) polypyridine-based biotinylation reagents.[6a] The much longer and more hydrophilic TEG spacer arm (ca. 23 Å) not only increases exposure of the biotin pendants but also reduces protein aggregation in an aqueous solution, which could facilitate recognition of the biotinylated biomolecules by avidin. It is worth mentioning that the titration results of bioconjugate **2-BSA** exhibited an equivalence point at [Ir]:[avidin] = ca. 2.5 and $-\Delta Abs_{500\ nm}$ = ca. 0.15 (Figure 7b). A deviation from the case of unmodified biotin is probably due to the substantial bulkiness of the biotinylated BSA molecule.

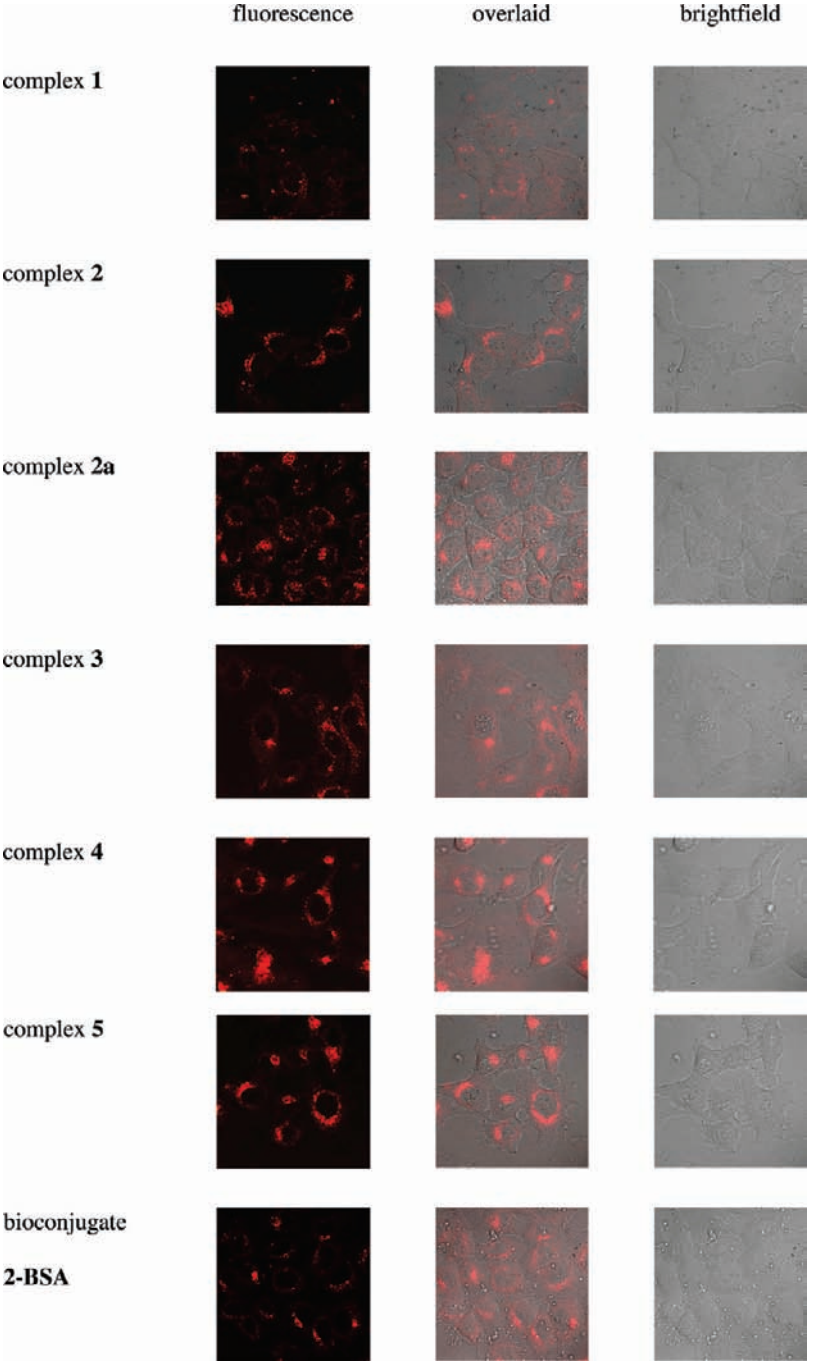

Figure 10. Microscopy images of HeLa cells incubated with the iridium(III) and rhodium(III) complexes (10 μM) and bioconjugate **2-BSA** ([Ir] = 10 μM) at 37 °C for 24 h.

Emission Titrations. The avidin-binding properties of the biotinylated models complex **2a** and bioconjugate **2-BSA** have been investigated by emission titrations. Since the biotinylated bioconjugates **1-BSA** and **3-BSA** did not show avidin binding in the HABA assays, they have been excluded in the emission titration studies. The titration results of complex **2a** are shown in Figures 8 and 9. This complex showed dual emission in an aerated aqueous phosphate buffer under ambient conditions. The emission spectrum was characterized by a dominant structured HE emission band at ca. 490 nm and a LE broad emission band at ca. 600 nm (Figure 8). The addition of avidin selectively reduced the emission intensity of the HE band by 72% and elongated the emission lifetimes (τ increased from 0.81 to 1.02 μs) without significantly altering the LE band. Thus, this led to a pronounced change of the emission profile of the complex (Figure 8). An equivalence point was observed at [avidin]:[Ir] = ca. 0.25 (Figure 9), which is in accordance with the result of the HABA assay (Figure 7a). Because the biotin-free complex $[Ir(ppy\text{-}CH_2NHC_4H_9)_2(bpy\text{-}Et)](PF_6)$ did not give similar observations,[30e] the changes of the emission properties of complex **2a** have been ascribed to its specific binding to avidin. Although the TEG spacer arm of complex **2a** is much longer than the depth of the biotin-binding site of the protein,[3b] the hydrophobic

nature of the $[Ir(N^{\wedge}C)_2(N^{\wedge}N)]^+$ complex core and the flexibility of the spacer arm would allow the luminescent unit to be close to the protein surface. This will result in a more hydrophobic local environment compared to a highly polar aqueous solution, leading to the changes of the photophysical properties of the complex. A similar "surface-binding" interaction has been reported for a biotin-spacer-dye compound and a transition-metal biotin complex.[40] The titration results of complex **2a** are similar to those of the dual-emissive biotin complex $[Ir(ppy\text{-}CH_2NHC_4H_9)_2(bpy\text{-}C6\text{-}biotin)](PF_6)$, which displayed a decrease of the emission intensity of the HE band at ca. 492 nm and a small emission enhancement of the LE shoulder at ca. 600 nm upon binding to avidin.[30e] In the current study, however, no substantial emission enhancement for the LE band of complex **2a** has been observed. Although we are not fully aware of the reasons for this finding, it should be due to an effect contributed by the TEG spacer arm because it is the only difference between complex **2a** and $[Ir(ppy\text{-}CH_2NHC_4H_9)_2(bpy\text{-}C6\text{-}biotin)](PF_6)$. In contrast to complex **2a**, bioconjugate **2-BSA** did not exhibit significant changes of the emission properties in the presence of avidin. It is likely that the biotinylated BSA is already hydrophobic in nature, and hence binding to avidin did not give a significant change of the local environment of the complex.

Cytotoxicity. The cytotoxicity of the cyclometalated iridium(III) and rhodium(III) complexes toward HeLa cells has been assessed by the MTT assay.[38] In our experiments, the survival of HeLa cells upon exposure to the complexes at various concentrations for 48 h was investigated and expressed in terms of IC_{50} values (Table 5). Complexes **1**−**3** exhibited relatively high IC_{50} values (57.8−61.4 μM), whereas those of the biotin-free complexes **4** (30.5 μM) and **5** (34.7 μM) were comparable to that of cisplatin (32.6 μM). It is interesting to note that complex **2** (IC_{50} = 61.4 μM) was less cytotoxic than complex **2a** (IC_{50} = 37.4 μM), which possesses two additional nonpolar *n*-butyl chains. It is likely that the lipophilicity of these complexes can be correlated to their cytotoxicity, with a more lipophilic complex being more cytotoxic. This is in agreement with the noncytotoxic nature of related cyclometalated iridium(III) bis- and tris-biotin complexes (IC_{50} > 400 μM), which are very hydrophilic because of the polar biotin pendants.[30h] Generally speaking, the cytotoxicity of these complexes is slightly lower than or comparable to that of other cyclometalated iridium(III) complexes appended with a long hydrocarbon chain or an indole moiety.[30f,g]

Live-Cell Imaging. The cellular uptake properties of the cyclometalated iridium(III) and rhodium(III) complexes **1**−**5** and the biotinylated bioconjugate **2-BSA** have been investigated using laser-scanning confocal microscopy. The microscopy images of HeLa cells incubated with these complexes and conjugate at 37 °C for 24 h are shown in Figure 10. Complexes **1**−**5** showed localization in the perinuclear region without significant uptake by the nucleus. Similar cellular staining has also been observed in the case of bioconjugate **2-BSA** (Figure 10). Additionally, the effects of the incubation temperature and the metabolic inhibitor CCCP[41] on the cellular uptake of complex **2a** and bioconjugate **2-BSA** have been investigated. Treatment of HeLa cells with complex **2a** at 4 °C did not reduce the cellular uptake efficiency (Figure 11). Also, incubation of the cells with CCCP at 37 °C in a glucose-free medium for 30 min before the addition of complex **2a** did not substantially alter the cellular uptake efficiency (Figure 11). These observations indicate that complex **2a** enters the cell mainly by energy-independent passive diffusion.[42] In contrast, the cellular uptake of bioconjugate **2-BSA** was suppressed (1) at low temperature and (2) upon treatment of the cells with CCCP (Figure 12), suggestive of an energy-dependent internalization pathway such as endocytosis. This is in accordance with the fact that uptake of BSA by HeLa cells occurs via receptor-mediated endocytosis.[43] We further investigated the subcellular distribution of bioconjugate **2-BSA** in HeLa cells by colocalization experiments using Alexa Fluor 633-labeled transferrin, which is an endocytic marker to track endosomes.[44] The microscopy images of HeLa cells treated with bioconjugate **2-BSA** and Alexa Fluor 633-labeled transferrin revealed partial overlap between the bioconjugate and transferrin-positive compartment (Figure S5 in the Supporting Information), indicative of the involvement of endosomes in trafficking of the

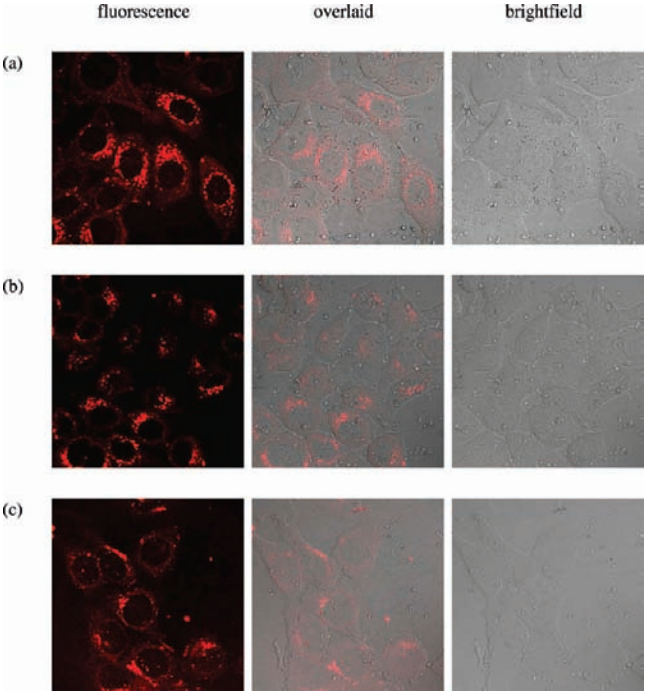

Figure 11. Microscopy images of HeLa cells incubated with complex **2a** (10 μM) for 3 h at (a) 37 °C, (b) 4 °C, and (c) 37 °C after the cells were preincubated with CCCP (20 μM) for 30 min.

(40) (a) Loosli, A.; Rusbandi, U. E.; Gradinaru, J.; Bernauer, K.; Schlaepfer, C. W.; Meyer, M.; Mazurek, S.; Novic, M.; Ward, T. R. *Inorg. Chem.* **2006**, *45*, 660–668. (b) Fürstenberg, A.; Kel, O.; Gradinaru, J.; Ward, T. R.; Emery, D.; Bollot, G.; Mareda, J.; Vauthey, E. *ChemPhysChem* **2009**, *10*, 1517–1532.

(41) Reaven, E.; Tsai, L.; Azhar, S. *J. Biol. Chem.* **1996**, *271*, 16208–16217.

(42) Hong, S.; Rattan, R.; Majoros, I.; Mullen, D. G.; Peters, J. L.; Shi, X.; Bielinska, A. U.; Blanco, L.; Orr, B. G.; Baker, J. R.; Banaszak Holl, M. M. *Bioconjugate Chem.* **2009**, *20*, 1503–1513.

(43) Weaver, D. J., Jr.; Voss, E. W., Jr. *Biol. Cell* **1998**, *90*, 169–181.

(44) (a) Dautry-Varsat, A.; Ciechanover, A.; Lodish, H. F. *Proc. Natl. Acad. Sci. U.S.A.* **1983**, *80*, 2258–2262. (b) Schmidt, U.; Briese, S.; Leicht, K.; Schürmann, A.; Joost, H.-G.; Al-Hasani, H. *J. Cell Sci.* **2006**, *119*, 2321–2331.

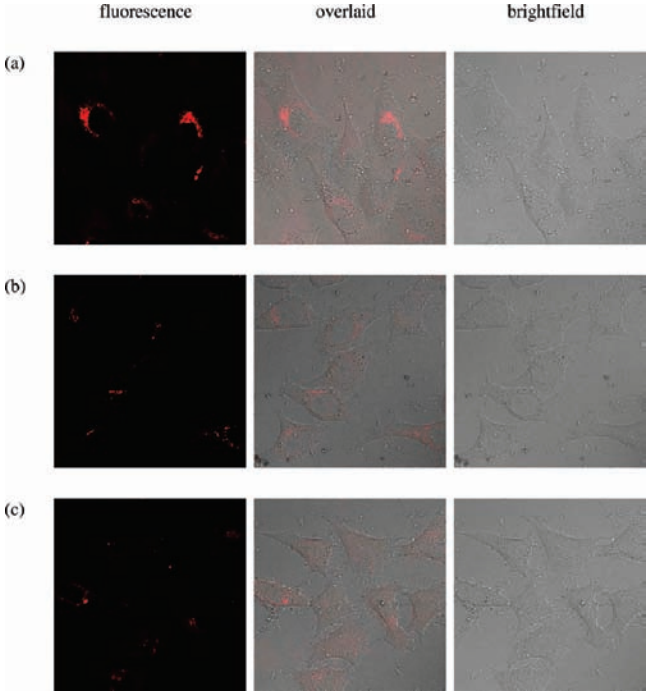

Figure 12. Microscopy images of HeLa cells incubated with bioconjugate **2-BSA** ([Ir] = 10 μM) for 2 h at (a) 37 °C, (b) 4 °C, and (c) 37 °C after the cells were preincubated with CCCP (20 μM) for 30 min.

luminescent bioconjugate and support of the proposed endocytic pathway. In general, subsequent localization of these luminescent species in the perinuclear region could be due to their interactions with lipophilic organelles such as the Golgi apparatus and endoplasmic reticulum.[45] More detailed studies will be required to fully understand the intracellular localization of the complexes and bioconjugates. Because both complex **2a** and bioconjugate **2-BSA** can serve as models for biomolecules that are biotinylated by complex **2**, their efficient cellular uptake demonstrates the possibility of utilizing these new luminescent biotinylation reagents in studies of the intracellular localization and trafficking of biological substrates and biomacromolecules.

(45) (a) Kobayashi, T.; Arakawa, Y. *J. Cell Biol.* **1991**, *113*, 235–244. (b) Pagano, R. E.; Martin, O. C.; Kang, H.-C.; Haugland, R. P. *J. Cell Biol.* **1991**, *113*, 1267–1279. (c) Haugland, R. P. *The Handbooks: A Guide to Fluorescent Probes and Labeling Technologies*, 10th ed.; Molecular Probes, Inc.: Eugene, OR, 2005; section 12. See: http://probes.invitrogen.com/handbook/sections/1200.html.

Conclusions

In this work, a new class of luminescent biotinylation reagents derived from cyclometalated iridium(III) and rhodium(III) bis(pyridylbenzaldehyde) complexes have been synthesized and their photophysical and electrochemical properties investigated. To examine the amine reactivity of the aldehyde groups, complex **2** has been reacted with a model primary amine, resulting in the formation of complex **2a**. The iridium(III) and rhodium(III) aldehyde complexes have been utilized to biotinylate BSA to give luminescent bioconjugates, the emissive and avidin-binding properties of which have been evaluated. In particular, the TEG spacer arm connecting the biotin pendant and the luminescent core allowed recognition of the biotinylated BSA by avidin. Interestingly, the dual-emissive complex **2a** revealed a pronounced change of the emission profile upon binding to avidin, rendering it a useful luminescent probe for the protein. The cytotoxicity of these complexes toward HeLa cells has been evaluated by the MTT assay. The cellular uptake characteristics of all of the complexes and the biotinylated bioconjugate **2-BSA** have been studied by laser-scanning confocal microscopy. Importantly, the complexes and the biotinylated bioconjugate showed efficient cellular internalization and retained their luminescence properties inside the cells. We anticipate that these new biotinylation reagents will contribute to the development of luminescent tracers for specific intracellular localization and trafficking of biological substrates and biomacromolecules.

Acknowledgment. We thank The Hong Kong Research Grants Council (Projects CityU 101908 and CityU 102109) for financial support. We thank Dr. Yun-Wah Lam and Mr. Yi-Min Liang for MALDI-TOF analysis. S.-K.L., K.Y.K., and K.Y.Z. acknowledge receipt of a Postgraduate Studentship administered by the City University of Hong Kong. K.Y.Z. also acknowledges receipt of a Research Tuition Scholarship and an Outstanding Academic Performance Award, both administered by the City University of Hong Kong.

Supporting Information Available: Evaluation of purification of the bioconjugates, MALDI-TOF MS analysis of unmodified BSA and bioconjugate **2-BSA**, HABA assays for complexes **1**−**3** in the absence and presence of BSA, and intracellular colocalization of bioconjugate **2-BSA** with an endocytic marker. This material is available free of charge via the Internet at http://pubs.acs.org.